Transition Met Chem (2012) 37:569–577
DOI 10.1007/s11243-012-9623-2

Synthesis, crystal structure, cytotoxicities and DNA-binding properties of a tetracopper(II) complex with *N*-benzoato-*N*′-[2-(2-hydroxyethylamino)ethyl-amino]oxamide ligand

Wen-Cai Chen · Ling-Dong Wang · Yan-Tuan Li · Zhi-Yong Wu · Cui-Wei Yan

Received: 20 April 2012 / Accepted: 8 June 2012 / Published online: 28 June 2012
© Springer Science+Business Media B.V. 2012

Abstract A new dissymmetrical *N,N*'-bis(substituted)-oxamide ligand, *N*-benzoato-*N*′-[2-(2- hydroxyethylamino)-ethyl]oxamide (H_3bhyox), and its tetranuclear copper(II) complex, $[Cu_4(bhyox)_2(dabt)_2](ClO_4)_2$ (**1**) have been synthesized and characterized (dabt = 2,2′-diamino- 4,4′-bithiazole). The crystal structures of H_3bhyox and complex **1** have been determined by X-ray single-crystal diffraction. Complex **1** has a cyclic tetranuclear cation with an embedded inversion center, in which the Cu–Cu separations through the oxamido and carboxyl bridges are 5.2246(6) and 5.3141(6) Å, respectively. Both Cu(II) centers at the inner and outer sites of the *cis*-bhyox^{3-} ligand have square pyramidal geometries. There is a 3D hydrogen-bonding network in the crystal. The cytotoxicities and DNA-binding properties of H_3bhyox and complex **1** were studied. Both compounds can interact with *HS*–DNA by intercalation, and the DNA-binding affinities are consistent with their in vitro cytotoxicities.

Electronic supplementary material The online version of this article (doi:10.1007/s11243-012-9623-2) contains supplementary material, which is available to authorized users.

W.-C. Chen · L.-D. Wang · Y.-T. Li (✉)
Marine Drug and Food Institute, Ocean University of China, 5 Yushan Road, Qingdao 266003, People's Republic of China
e-mail: yantuanli@ouc.edu.cn

Z.-Y. Wu
Key Lab. Marine Drug, Chinese Minist. Educ., Ocean University of China, Qingdao, People's Republic of China

C.-W. Yan (✉)
College of Marine Life Science, Ocean University of China, Qingdao 266003, People's Republic of China
e-mail: cuiweiyan@ouc.edu.cn

Introduction

DNA is the primary target for many anticancer drugs since it contains all the genetic information required for cellular function [1]. Cisplatin is one of the most successful drugs used in the clinic for the treatment of testicular, bladder, lung, and ovarian cancers and has been shown to act on DNA by numerous studies [2]. Despite its remarkable pharmacological activity, cisplatin has severe disadvantages such as a relatively limited spectrum of activity and high toxicity [3]. With the hope of finding highly effective, target-specific and less toxic drugs, much effort has been devoted to the development of metal-based anticancer agents in recent years. Transition metal complexes can interact with DNA by noncovalent modes such as intercalation, groove binding, and electrostatic effects. Intercalation has attracted special interest due to its various applications in cancer therapy and molecular biology [4, 5]. In general, the intercalating ability not only correlates with the planarity of a ligand but is also related to the coordination geometry of the metal center and donor atom types of the ligand [6]. In addition, both the type of metal and its valency play important roles in deciding the binding extent of complexes to DNA [7]. Many copper(II) complexes have been studied in this context, since copper, as a biologically active metal, has many correlations with endogenous oxidative DNA damage associated with aging and cancer [8]. Compared to mono- and binuclear copper(II) complexes [9, 10], relatively few studies on tetranuclear copper(II) complexes have been reported to date [11]. However, the reported enhancement of DNA-binding activity and cytotoxicities for tetranuclear complexes prompted us to design and synthesize new tetracopper(II) complexes.

A promising strategy to design and synthesize polynuclear complexes is the use of bridging ligands. In this regard, *N,N'*-bis(substituent)oxamides have played a key role as bridging ligands because their coordinating ability toward transition metals can be modified by varying the amide substituents. Following this synthetic approach, a series of polynuclear complexes with interesting structures based the bridging symmetrical *N,N′*-bis(substituted)oxamides have been reported [12, 13]. However, the studies on dissymmetrical *N,N'*-bis(substituted)oxamides are limited [14], due to the difficulties of their synthesis. We therefore decided to synthesize new tetracopper(II) complexes with bridging dissymmetrical *N,N'*-bis(substituted)oxamides in order to evaluate the factors effecting their DNA-binding properties and cytotoxicities.

With these thoughts in mind, in this paper, a new dissymmetrical *N,N'*-bis(substituted)oxamide ligand, namely *N*-benzoato-*N′*-[2-(2-hydroxylethylamino)ethyl]oxamide (H_3bhyox), and its tetracopper(II) complex, $[Cu_4(bhyox)_2(dabt)_2](ClO_4)_2$ (**1**) (dabt = 2,2′-diamino-4,4′-bithiazole) have been synthesized and structurally characterized by single-crystal X-ray diffraction. In vitro cytotoxicities and the reactivities toward DNA of the two compounds are reported.

Experimental

Materials and measurements

Ethidium bromide (EB) and herring sperm DNA (HS–DNA) were purchased from Sigma Corp. and used as received. All other chemicals were of reagent grade and obtained commercially.

The C, H, and N microanalyses were obtained on a Perkin-Elmer 240 elemental analyzer. Molar conductances were measured with a Shanghai DDS-11A conductmeter. Mass spectra (ES-MS) were measured with a Waters Q-TOF GLOBLE mass spectrometer. NMR spectra were recorded with a JEOL-ECP 600 spectrometer with TMS as internal standard and DMSO-d_6 as solvent, and chemical shifts are reported as δ values. IR spectra were recorded on a Nicolet-470 spectrophotometer in the range 4,000–400 cm^{-1} as KBr pellets. Electronic spectra (in DMF) were recorded on a Cary 300 spectrophotometer. Fluorescence spectra were measured with an Fp-750w Fluorometer. Viscosity experiments were carried out using an Ubbelodhe viscometer maintained at a constant temperature of 298.0 (±0.1) K in a thermostatic water bath.

Caution: Although we have not encountered any problems, perchlorate compounds are potentially explosive and should be handled with care.

Synthesis of H_3bhyox

A solution of ethyl oxalyl chloride (1.11 mL, 10 mmol) in THF (10 mL) was added dropwise to a solution of anthranilic acid (1.37 g, 10 mmol) in THF (mL) at 273 K. The mixture was stirred rapidly for 1 h at room temperature, and then, absolute ethanol (20 mL) was added. After 0.5 h, the mixture was added dropwise to a solution of 2-(2-aminoethylamino)ethanol (1.1 mL, 10 mmol) in absolute ethanol (20 mL) at 273 K. The resulting solution was stirred for 8 h, whereupon H_3bhyox precipitated as a white powder which was filtered off, washed with absolute ethanol and dried under vacuum. Yield: 2.33 g (79 %). Colorless crystals of H_3bhyox suitable for X-ray analysis were obtained from an ethanol/water (3:2) mixture by slow evaporation for 2 weeks at room temperature. Anal. Calc. for $C_{13}H_{20.4}N_3O_{5.7}$(%): C, 47.8; H, 6.3; N, 12.8. Found(%): C, 47.7; H, 6.2; N, 12.9. IR (KBr pellet, cm^{-1}): 3,311 [ν(O–H)]; 1,675 [ν(C=O)]. ES-MS, m/z (%): 296.1(100) $[M + H]^+$. ^{1}H NMR (600 MHz, DMSO-d^6, δ, ppm): 14.65 (s, 1H), 8.99 (*t*, $J = 5.82$ Hz, 1H), 8.53 (*d*, $J = 2.28$ Hz, 1H), 8.00 (dd, 1H), 7.37 (*d*, $J = 3.36$ Hz, 1H), 7.08 (*s*, 1H), 5.92 (*m*, 1H), 3.69 (*m*, 2H), 3.32 (*m*, 4H), 2.50 (*m*, 4H), 1.92 (*m*, 2H).

Synthesis of complex **1**

To a stirred solution of $Cu(ClO_4)_2{\cdot}6H_2O$ (0.0371 g, 0.1 mmol) in ethanol (5 mL), a solution of H_3bhyox (0.0148 g, 0.05 mmol) and piperidine (0.0128 g, 0.15 mmol) in ethanol (10 mL) was added dropwise at room temperature. After stirring for 0.5 h, a solution of dabt (0.0099 g, 0.05 mmol) in ethanol (5 mL) was added dropwise. The mixture was stirred vigorously at 333 K for 5 h, the resulting green solution was filtered and green cube crystals of the complex suitable for X-ray analysis were obtained by slow evaporation at room temperature. Yield: 0.0330 g (64 %). Anal. Calc. for $Cu_4C_{38}H_{40}N_{14}O_{18}S_4Cl_2$ (%): C, 31.8; H, 2.7; N, 13.7. Found(%): C, 31.8; H, 2.8; N 13.6. IR (KBr pellet, cm^{-1}): 1,632 [ν(C=O) + ν_{as}(COO)]; 1,365 [ν(C=N)]; 1,107, 623 [$\nu(ClO_4)$]. Molar conductance: Λ_M (DMF solution): 146 Ω^{-1} cm^{-2} mol^{-1}. ES-MS, m/z (%): 1,236.2 (100) $[M\text{-}2ClO_4]^+$.

X-ray crystallography

The X-ray diffraction experiments were made on a Bruker APEX area-detector diffractometer with graphite monochromatic Mo−Kα radiation ($\lambda = 0.71073$ Å) at 296 K. The crystal structures were solved by direct methods followed by Fourier syntheses. Structure refinement was performed by full matrix least-squares procedures using SHELXL-97 on F^2 [15]. For the free ligand, the H atoms on

Table 1 Crystal data and details of the structure determination for *H3bhyox* (**L**) and complex **1**

Empirical formula	$C_{13}H_{17}N_3O_5 \cdot 1.7(H_2O)$ **(L)**	$C_{38}H_{40}Cu_4N_{14}O_{10}S_4 \cdot 2(ClO_4)$**(1)**
Formula weight	325.92	1,434.22
Crystal system	Monoclinic	Monoclinic
Space group	P2(1)/*n*	C2/c
Unit cell dimensions (Å °)		
a	12.7747(2)	14.0035(13)
b	19.1528(3)	24.654(2)
c	14.0693(2)	15.5419(14)
α	90.00	90
β	110.287(1)	105.501(2)
γ	90.00	90
Volume ($Å^3$), *Z*	3,228.82(9), 8	5,170.6(8), 4
D(calc) (g cm^3)	1.341	1.842
μ (MoKα) (mm^{-1})	0.109	1.975
F(0 0 0)	1,384	2,896
Crystal size (mm^3)	0.30 0.25 0.15	0.10 × 0.25 × 0.30
Radiation (Å) (Mo−Kα)	0.71073	0.71073
θ range	1.9–27.7	1.65–27.59
Tot., uniq. data	16,369, 7,546, 0.030	15,316, 5,926, 0.0351
Observed data [$I > 2\delta(I)$]	4,361	4,260
R indices	0.0606, 0.2091	0.0403, 0.1099
S	1.02	1.022
Max., av.	0.00/0.00	0.00/0.00

nitrogen and oxygen atoms were located in a difference Fourier map (DFP) and refined freely for N atoms or treated as riding for O atoms, with $U_{iso}(H) = 1.5\ U_{eq}$ (waters). H atoms on C atoms were placed in calculated positions, with C–H = 0.93 (aromatic), 0.97 Å (methylene), and refined in riding modes, with $U_{iso}(H) = 1.2\ U_{eq}$ (carrier atoms). For complex **1**, the H atoms on nitrogen and oxygen atoms were found in a DFP and then refined with a riding model (atoms O5, N6 and N7) or freely (atom N3). Other H atoms on carbon atoms were treated as for the ligand. Crystal data and structure refinement parameters are summarized in Table 1.

In vitro cytotoxicity evaluation

In vitro cytotoxicities of the free ligand (H_3bhyox), complex **1** and cisplatin were evaluated against two cancer cell lines including SMMC-7721 and A549 using the Sulforhodamine B (SRB) assay. All cells were cultured in RPMI 1640 supplemented with 10 % (v/v) fetal bovine serum, 1 % (w/v) penicillin (104 U/mL) and 10 mg/mL streptomycin. Cell lines were maintained at 310 K in a 5 % (v/v) CO_2 atmosphere with 95 % (v/v) humidity. Cultures were passaged weekly using trypsin–EDTA to detach the cells from their culture flasks. The two compounds and cisplatin were dissolved in DMSO and diluted to the required concentration with culture medium before use. The content of DMSO in the final concentrations did not exceed 0.1 %. At this concentration, DMSO was found to be non-toxic to the cells tested. Rapidly growing cells were harvested, counted, and incubated at the appropriate concentration in 96-well microplates for 24 h. The test two compounds dissolved in culture medium were then applied to the culture wells to achieve final concentrations ranging from 10^{-3} to 10^2 μg/mL. Control wells were prepared by addition of culture medium without cells. The plates were incubated at 310 K in a 5 % CO_2 atmosphere for 48 h. Upon completion of the incubation, the cells were fixed with ice-cold 10 % trichloroacetic acid (100 mL) for 1 h at 277 K, washed five times with distilled water and allowed to dry in the air, then stained with 0.4 % SRB in 1 % acetic acid (100 mL) for 15 min. The cells were washed four times with 1 % acetic acid and air-dried. The stain was solubilized in 10 mM unbuffered Tris base (100 mL) and the OD of each well was measured at 540 nm on a microplate spectrophotometer. The IC_{50} values were calculated from the curves constructed by plotting cell survival (%) versus the concentrations of the test compound.

DNA-binding studies

All experiments involving Herring Sperm DNA (HS–DNA) were performed in tris-(hydroxymethyl)aminomethane-HCl (Tris–HCl) buffer solution (pH = 7.35). Tris–HCl buffer was prepared using deionized and sonicated triple distilled water. The solution of HS–DNA in Tris–HCl buffer gave a ratio of UV–visible absorbance at 260 and 280 nm, A_{260}/A_{280}, of ca. 1.9, indicating that the DNA was sufficiently free of protein. The concentration of HS–DNA was determined by UV–visible absorbance at 260 nm. The molar absorption coefficient, ε_{260}, was taken as 6,600 $M^{-1}\ cm^{-1}$. Stock solution of HS–DNA was stored at 277 K and used after no more than 3 days. Concentrated stock solutions of the compounds were prepared by dissolving samples in DMSO and diluted suitably with Tris–HCl buffer to the required concentrations. Absorption spectral titrations were performed by keeping the concentration of the test compound constant while varying the HS–DNA concentration. Equal solutions of HS–DNA were added to the test compound and reference solutions to eliminate the absorbance of HS–DNA itself. In the ethidium bromide (EB) fluorescence displacement experiments, 5 μL of EB Tris–HCl solution (1 mM) was added to 1 mL of HS–DNA solution (at saturated binding levels), and the mixture stored in the dark for 2 h, then titrated into the DNA/EB mixture and diluted in Tris–HCl buffer to 5 mL, producing a set of solutions with varying

mole ratio of the test compound to HS–DNA. Before measurement, the mixture was shaken and incubated at room temperature for 30 min. The fluorescence spectra were obtained at an emission wavelength of 584 nm in the fluorometer. For the viscosity measurements, HS–DNA samples approximately 200 base pairs in length were prepared by sonication in order to minimize complexities arising from DNA flexibility. Flow times were measured with a digital stopwatch. Each sample was measured three times, and an average flow time was calculated. Relative viscosities for HS–DNA in the presence and absence of the test compounds were calculated from the relation $\eta = (t - t_0)/t_0$, where t is the observed flow time of DNA-containing solution and t_0 is that of Tris–HCl buffer alone. Data were analyzed as $(\eta/\eta_0)^{1/3}$ versus binding ratio, where η is the viscosity of DNA in the presence of the compound and η_0 is the viscosity of DNA alone.

Results and discussion

Synthesis and properties

The new ligand, N-benzoato-N′-[2-(2-hydroxyethylamino)ethyl]oxamide (H_3bhyox), is expected to function as a bridging ligand because it may coordinate to metals through not only its oxamido oxygens and nitrogens but also the oxygens of the carboxyl group. In this work, 2,2′-diamine-4,4′-bithiazole (dabt) was used as terminal co-ligand. In order to prepare complex **1**, the use of piperidine as base allows the bridging ligand (H_3bhyox) to coordinate to copper(II) through the deprotonated oxamido nitrogen atoms. Elemental analyses indicate that the reaction of H_3bhyox with $Cu(ClO_4)_2{\cdot}6H_2O$ plus dabt yielded the tetracopper(II) complex $[Cu_4(bhyox)_2(dabt)_2](ClO_4)_2$ (**1**). The synthetic pathway for H_3bhyox and complex **1** are shown in Scheme 1.

H_3bhyox is soluble in water, DMF and DMSO, and slightly soluble in methanol and ethanol at room temperature. Complex **1** is insoluble in common polar solvents, but very soluble in DMF and DMSO to give stable solutions at room temperature, consistent with its polymeric nature [16]. The molar conductance value (146 Ω^{-1} cm^{-2} mol^{-1}) of complex **1** in DMF solution falls in the expected range for a 1:2 electrolyte [17], suggesting that the tetracopper(II) complex consists of a tetracopper(II) complex cation $[Cu_4(bhyox)_2(dabt)_2]^{2+}$ and two uncoordinated perchlorate anions in solutions. The stability of complex **1** as a whole tetranuclear entity in solution was further supported by the ES-MS results (see "Experimental").

Spectroscopic characterization

Comparison of the IR spectra of free H_3bhyox and its tetracopper(II) complex provide some information regarding the mode of coordination in the tetra- copper(II) complex. It is noteworthy that the antisymmetric stretching vibration of the carboxylate group [$\nu_{as(COO)}$], together with the carbonyl stretching vibration of the oxamidate group ($\nu_{C=O}$) of the free H_3bhyox at 1,675 cm^{-1} are considerably shifted toward lower frequency (1,632 cm^{-1}) in the

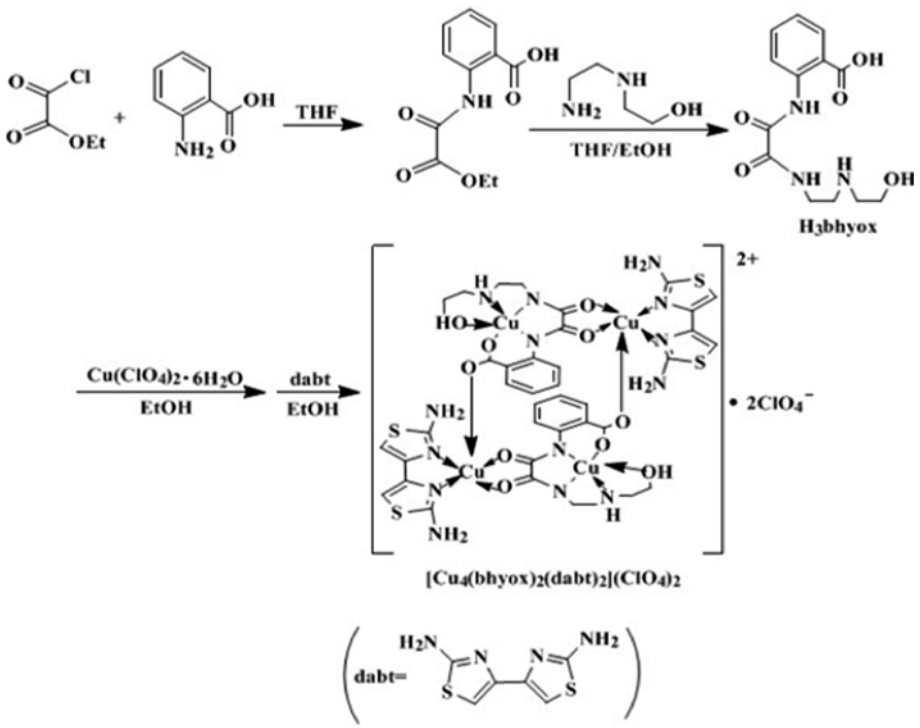

Scheme 1 The synthetic pathway for H_3bhyox and complex **1**

complex, implying that not only the oxygens of the oxamidate group but also the oxygens of the carboxylate group are coordinated with copper(II) to form a tetranuclear complex [18]. In addition, the skeletal vibration of the bithiazole is reasonably red-shifted, being observed at 1,365 cm^{-1} in complex **1**, indicating that the dabt ligand is involved in terminal coordination to the tetracopper(II) complex [19]. Furthermore, a broad and intense band centered at 1,088 cm^{-1}, plus a strong sharp band at 624 cm^{-1} assigned to the antisymmetric and antisymmetric bending vibrations of the non-coordinated perchlorate group [20] are also observed for complex **1**.

The electronic spectrum of the tetracopper(II) complex was recorded in the UV–Vis region (200–800 nm). Spectra obtained for complex **1** at different concentrations (1.6×10^{-5} to 6×10^{-6} M in DMSO) obeyed the Beer-Lambert law, indicating that the tetracopper(II) complex stays intact at these concentrations. The complex shows two absorption bands, the band at 230 nm ($\varepsilon = 8.02 \times 10^4$ M^{-1} cm^{-1}) can be assigned to the $\pi-\pi^*$ transition of the coordinated oxamide group. The second, broad band at 671 nm ($\varepsilon = 697$ M^{-1} cm^{-1}) is assigned to the *d–d* transition of copper(II) [21]. For the free ligand H_3bhyox, there is an intense band at 231 nm and a less intense band at 276 nm which can be assigned to the intramolecular and intermolecular $\pi-\pi^*$ transitions of the substituted benzene ring, respectively.

Crystal structure of H_3bhyox

As shown in Fig. 1a, the asymmetric unit of H_3bhyox contains two molecules [$\mathbf{L_A}$ (C1–C13) and $\mathbf{L_B}$ (C14–C26)] plus 3.4 solvent water molecules. Both H_3bhyox molecules are in the *trans*- conformation; the torsion angles C9–N2–C10–C11 and C22–N5–C23–C24 are 68.4(3)° and 74.9(3)°, respectively. The torsion angles of N2–C10–C11–N3 [61.4(3)°] and N5–C23–C24–N6 [64.6(3)°] indicate gauche conformations for the bonds C10–C11 and C23–C24. $\mathbf{L_A}$ and $\mathbf{L_B}$ form a dimer as shown in Fig. 1b. In this array, each molecule has four sites interacting with its neighbor, by two classical hydrogen bonds, one non-classical hydrogen bond (Table 2) and one π–π stacking interaction. The benzene rings of $\mathbf{L_A}$ and $\mathbf{L_B}$ subtend a dihedral angle of 7.78(18)° and the distance between ring centroids is 4.1182(16) Å.

The molecule pairs link each other to form a chain parallel to the [1 0 −1] direction via the hydrogen bonds involving hydroxyl groups [N3–H3B···O10^{i} and O5–H5C···O2^{i}, symmetry code (i) = $x + 1/2, 1/2 - y, z - 1/2$. Fig. S1].

Crystal structure of complex **1**

The complex consists of a centrosymmetric tetranuclear cation and two uncoordinated perchlorate anions

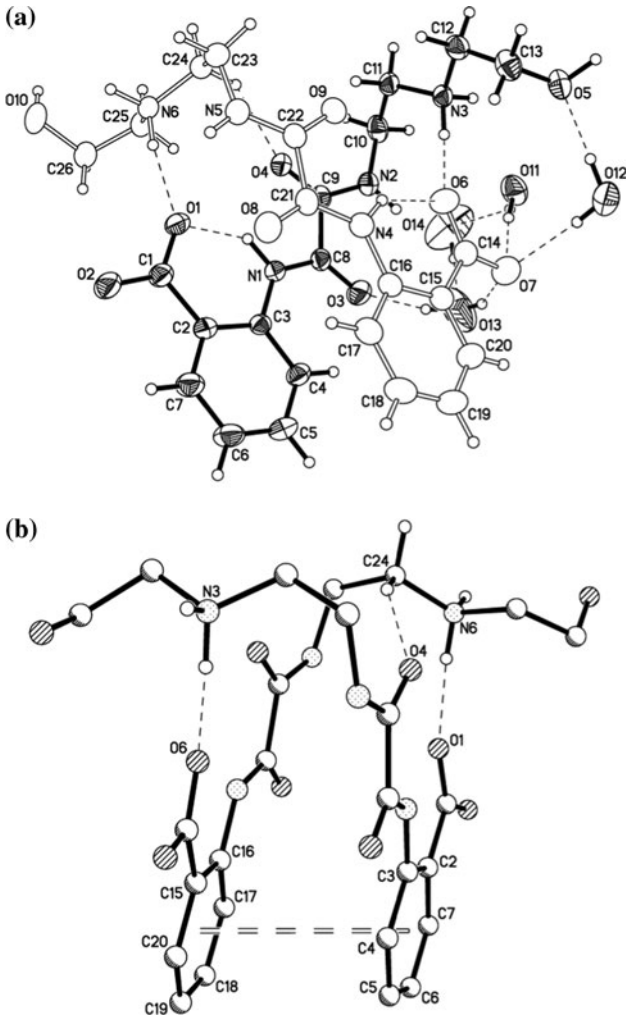

Fig. 1 **a** An ORTEP view of ligand **L** with the thermal ellipsoids at 30 % probability level. H atoms are shown as small spheres of arbitrary radii. Hydrogen bonds are shown as *dotted lines*. **b** A view of the couple formed by $\mathbf{L_A}$ and $\mathbf{L_B}$. In such an array, the ligand molecules, respectively have five sites interacting with each other [two classical hydrogen bonds, two non-classical hydrogen bonds, one π–π stacking interaction]

(Fig. 2a). The Cu–Cu separations through the oxamido and the carboxyl bridges are 5.2246(6) and 5.3141(6) Å, respectively. The octadentate bhyox^{3-} ligand adopts a *cis*-conformation. Both the inner and the outer copper(II) centers (atoms Cu1 and Cu2, respectively) are in square pyramidal coordination geometries with τ values [22] of 0.03 and 0.06, respectively. Atom Cu1 in an $\{N_3O_2\}$ environment is displaced from the basal plane (O1, N1, N2 and N3) 0.1965(13) Å forward the apical hydroxyl group (O5). The Cu1–N3 bond is longer than Cu1–N1 and Cu1–N2 (Table 3), which is consistent with the stronger donor abilities of the deprotonated amide N atoms compared to the primary amine N atoms. Atom Cu2 has an $\{N_2O_3\}$ coordination and deviates 0.1629(12) Å from the basal plane.

Table 2 Hydrogen-bonding geometries (Å °) for the ligand

D–H···A	d(D–H)	d(H···A)	d(D···A)	<(DHA)
N1–H1A···O1	0.96(3)	1.84(3)	2.625(3)	137(2)
N3–H3A···O6	0.98(3)	1.80(3)	2.774(3)	172(3)
N3–H3B···O10^{i}	0.88(3)	2.04(3)	2.789(3)	142(3)
N4–H4A···O6	0.94(3)	1.78(3)	2.576(3)	141(2)
N5–H5A···O12^{ii}	0.88(3)	2.33(3)	3.033(3)	136(2)
N6–H6A···O1	0.93(3)	1.85(3)	2.747(3)	161(2)
N6–H6A···O11^{ii}	0.97(3)	1.97(3)	2.867(3)	153(2)
O5–H5B···O2^{i}	0.96	1.66	2.614(3)	173.4
O10–H10C···O12^{iii}	0.96	1.77	2.726(3)	164.7
O11–H11C···O7	0.93	1.89	2.814(3)	171.2
O11–H11D···O14	0.99	2.16	2.989(6)	140.8
O12–H12C···O5	0.94	1.81	2.756(3)	178.4
O12–H12D···O7	0.88	1.97	2.832(3)	168.8
O13–H13C···O3	0.86	2.06	2.889(5)	160
O13–H13D···O7	0.92	2.31	3.170(7)	155.4
O14–H14C···O2^{iv}	0.88	2.25	3.033(6)	146.9
O14–H14D···O13	0.87	1.82	2.636(10)	155.9
C24–H24B···O4	0.97	2.41	3.291(3)	150.9
C25–H25A···O8^{v}	0.97	2.50	3.375(4)	149.3

Symmetry codes: (i) $x + 1/2, 1/2 - y, z - 1/2$; (ii) $x - 1/2, 1/2 - y, z + 1/2$; (iii) $x, y, z + 1$; (iv) $x + 1, y, z$; (v) $x + 1/2, 1/2 - y, z + 1/2$

Around atom Cu1, the five-membered chelate rings (Cu1–N2–C10–C11–N3 and Cu1–N3–C12–C13–O5) have envelope conformations with the Pucker parameters [23] of $Q = 0.418(3)$ Å, $\varphi = 115.8(4)°$ and $Q = 0.491(3)$ Å, $\varphi = 65.7(3)°$, respectively. The six-membered chelate ring formed by the carboxylato group folds 16.32(12)° along C1···N1 ($Q = 0.232(3)$ Å, $\theta = 82.2(7)°$ and $\varphi = 292.0(6)°$). The carboxylate group bridges the copper(II) centers in a skew–skew fashion, with torsion angles of Cu1–O1–C1–O2 = 163.4(2)°and Cu2^{i}–O2–C1–O1 = −94.7(3)° [symmetry code: (i) = $1/2 - x, 1/2 - y, 1 - z$], which are similar to those found in related complexes [24].

In the crystal, the tetranuclear cations and the perchlorate anions make up a hydrogen-bonding network parallel to the *bc* plane (Fig. S3, Table 4). Moreover, the cations form a chain extending along the [1 0 1] direction through the hydrogen bonds between the hydroxyl and carboxylate groups (Fig. 2b). Finally, the networks and chains together complete a three-dimensional supramolecular structure.

In vitro cytotoxicities

In vitro cytotoxicities of the two compounds together with cisplatin against two cancer cell lines, namely human hepatocellular carcinoma cell line SMMC-7721 and human lung adenocarcinoma cell line A549 were conducted in our study. The results indicate that the free ligand H_3bhyox has no cytotoxicities against the two cancer cell lines, whereas

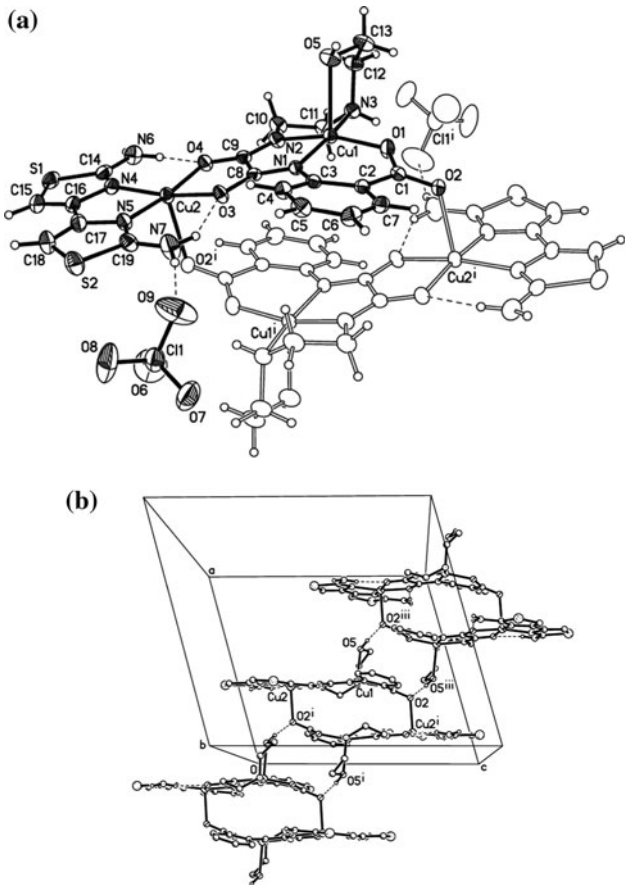

Fig. 2 **a** An ORTEP view of complex **1** with the thermal ellipsoids at 30 % probability level. H atoms are shown as small spheres of arbitrary radii. Hydrogen bonds are shown as *dotted lines*. Symmetry codes: (i) = $1/2 - x$, $1/2 - y$, $1 - z$. **b** A view of the one-dimensional hydrogen-bonding structure parallel to [1 0 1] direction. Symmetry codes: (i) = $1/2 - x, 1/2 - y, 1 - z$; (iii) = $1 - x, y, 3/2 - z$

complex **1** displayed significant cytotoxicities with IC_{50} values of 22.0 ± 0.4 and 36.0 ± 0.6 μg/mL for SMMC-7721 and A549, respectively. Though the in vitro cytotoxicities for complex **1** are less than those of cisplatin (IC_{50} values of 5.4 and 7.6 μg/mL, respectively), the inhibition of cell proliferation produced by complex **1** is still rather active. According to these results, we conclude that complexation may be the major cause of the enhanced effect on the viability of cancer cells [25]. These findings encouraged us to explore the DNA-binding properties of the two compounds.

UV–visible absorption titration

Electronic absorption spectroscopy is widely used to study the binding modes of metal complexes with DNA. Generally, the observations of hypochromism and red-shift caused by adding DNA to solutions of test compounds, are attributed to intercalation of the aromatic chromophore of the test compound between the base pairs of DNA [26].

Table 3 Selected bonds (Å) and angles (°) for the complex **1**

Cu1–N1	1.972(2)	Cu1–N2	1.920(2)
Cu1–N3	2.047(3)	Cu1–O1	1.909(2)
Cu1–O5	2.371(2)	Cu2–N4	1.965(3)
Cu2–N5	1.981(3)	Cu2–O2^{i}	2.345(2)
Cu2–O3	1.968(2)	Cu2–O4	1.959(2)
O1–Cu1–O5	96.63(10)	O1–Cu1–N1	93.78(9)
O1–Cu1–N2	163.55(11)	O1–Cu1–N3	97.80(11)
O5–Cu1–N1	108.86(9)	O5–Cu1–N2	99.48(10)
O5–Cu1–N3	78.33(10)	N1–Cu1–N2	84.14(10)
N1–Cu1–N3	165.61(11)	N2–Cu1–N3	82.34(11)
O2^{i}–Cu2–O3	90.69(8)	O2^{i}–Cu2–O4	94.87(9)
O2^{i}–Cu2–N4	100.38(9)	O2^{i}–Cu2–N5	92.97(10)
O3–Cu2–O4	84.00(8)	O3–Cu2–N4	168.79(10)
O3–Cu2–N5	95.07(10)	O4–Cu2–N4	96.75(10)
O4–Cu2–N5	172.11(11)	N4–Cu2–N5	82.64(11)
Cu1–O1–C1–O2	163.4(2)	Cu2^{i}–O2–C1–O1	−94.7(3)

Symmetry code: (i) = 1/2 − x, 1/2 − y, 1 − z

Table 4 Hydrogen-bonding geometries (Å °) for the complex **1**

D–H···A	d(D–H)	d(H···A)	d(D···A)	<(DHA)
N6–H6A···O4	0.85	2.14	2.890(4)	146.2
N6–H6B···O7^{ii}	0.87	2.39	3.094(4)	137.8
N7–H7A···O3	0.89	2.05	2.858(4)	149.1
N7–H7B···O9	0.89	2.02	2.890(4)	167.3
O5–H5···O2^{iii}	0.87	1.85	2.718(3)	173.9

Symmetry codes: (ii) = 1/2 − x, y − 1/2, 1/2 − z; (iii) = 1 − x, y, 3/2 − z

The absorption plots of H_3bhyox and its complex in the absence and presence of HS–DNA are given in Figs. 3 and 4, respectively. As shown in the two figures, when titrated with HS–DNA, both compounds presented significant hypochromism accompanied by slight red-shifts of 1 nm in the absorbance maxima. These characteristics reveal that both compounds interact with HS–DNA most likely through the intercalation mode [27].

For the purpose of quantitatively evaluating the binding strength of the two compounds with HS–DNA, the intrinsic binding constants K_b were determined by monitoring the changes in absorbance at 276 nm for H_3bhyox and 230 nm for the complex, using the following equation [27]:

$$[\mathrm{DNA}]/(\varepsilon_a - \varepsilon_f) = [\mathrm{DNA}]/(\varepsilon_b - \varepsilon_f) + 1/K_b((\varepsilon_b - \varepsilon_f)) \quad (1)$$

where [DNA] is the concentration of DNA, ε_f, ε_a and ε_b correspond to the extinction coefficients, respectively, for the free compounds, for each addition of HS–DNA to their solutions and for the compounds in the fully bound form. From the plots of [DNA]/(ε_a − ε_f) versus [DNA] (insets in Fig. 4), the binding constants for free H_3bhyox and the

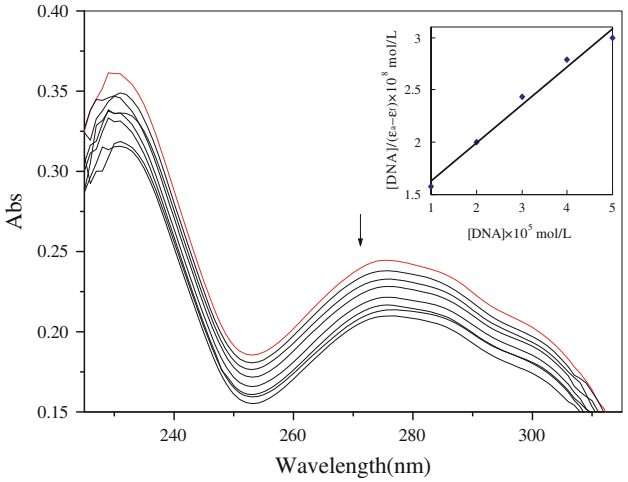

Fig. 3 Absorption spectra of ligand **L** upon the titration of *HS*–DNA. *Arrow* indicates the change upon increasing the DNA concentration. *Inset* Plot of [DNA]/(ε_a – ε_f) versus [DNA] for the absorption titration of *HS*–DNA with ligand

complex were calculated as 4.00 × 10^4 M^{-1} (r = 0.9962 for five points) and 6.67 × 10^4 M^{-1} (r = 0.9984 for six points), respectively. These K_b values are lower than those observed for classical intercalators (e.g. EB, ∼10^6 M^{-1}) [28], but are similar to those of some well-established intercalation agents (∼10^4 M^{-1}) [29, 30]. The binding ability of complex **1** is better than that of the free ligand **L**. This may be mainly due to the contribution of the thiazole rings of the terminal ligands in the complex, which are expected to be stacked between base pairs upon interaction with DNA. Electrostatic interactions may be another factor for the complex to enhance the binding strength to DNA compared to H_3bhyox alone [8].

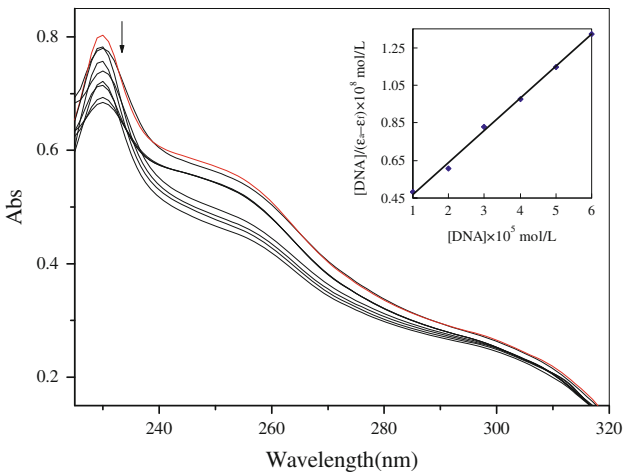

Fig. 4 Absorption spectra of complex **1** upon the titration of *HS*–DNA. *Arrow* indicates the change upon increasing the DNA concentration. *Inset* Plot of [DNA]/(ε_a – ε_f) versus [DNA] for the absorption titration of *HS*–DNA with the complex

Fluorescence titration

In order to further investigate the interaction modes of the two compounds with HS–DNA, ethidium bromide fluorescence displacement experiments were carried out. For test compounds that intercalate into DNA, the binding sites of DNA available for EB will be reduced, and hence the fluorescence intensity of EB will be quenched [31]. In our experiments, as illustrated in Figs. 5 and 6, the fluorescence intensities of EB bound to DNA at 584 nm show a notable decrease with increasing concentrations of the two compounds, indicating that some EB molecules were delivered into solution after an exchange with the test compounds, resulting in fluorescence quenching of EB. This observation is often the characteristic of intercalation.

In order to understand quantitatively the magnitude of the binding strength of the two compounds with HS–DNA, the linear Stern–Volmer equation was employed [31]:

$$I_0/I = 1 + K_{sv}[Q] \quad (2)$$

where I_0 and I represent the fluorescence intensities in the absence and presence of quencher, respectively. K_{sv} is the linear Stern–Volmer quenching constant, and Q is the concentration of quencher. In the quenching plots (inset in Figs. 5, 6, respectively) of I_0/I versus [compound], the K_{sv} values are given by the ratio of the slope to intercept. The K_{sv} values for H_3bhyox and the complex are 1.97×10^4 ($r = 0.9985$ for five points) and 1.02×10^5 ($r = 0.9940$ for seven points), respectively. The order of these values is consistent with the results derived from the absorption spectra.

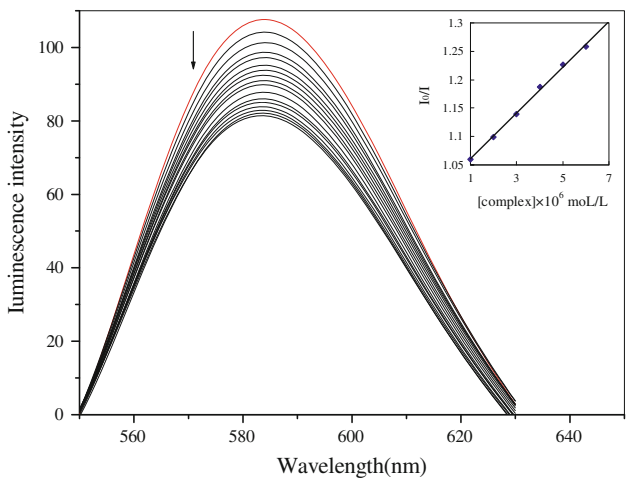

Fig. 5 Emission spectra of the *HS*–DNA–EB system upon the titration of ligand **L**. *Arrow* shows the change upon the increasing ligand concentration. Inset: Plot of I_0/I versus [ligand] for the titration of the ligand to *HS*–DNA–EB system

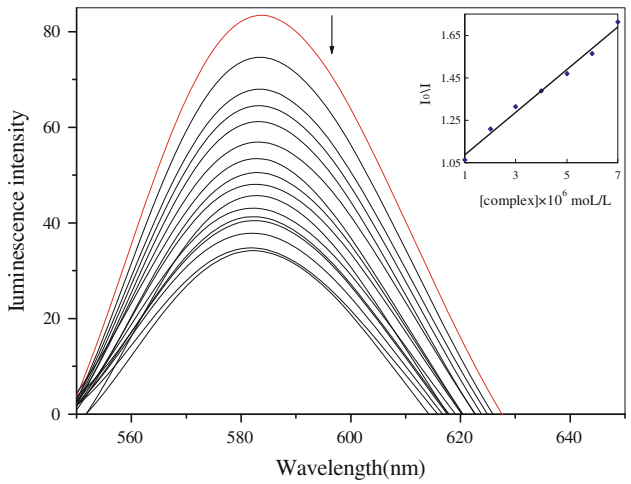

Fig. 6 Emission spectra of the *HS*–DNA–EB system upon the titration of complex **1**. *Arrow* shows the change upon the increasing complex **1** concentration. *Inset* Plot of I_0/I versus [complex] for the titration of the complex to *HS*–DNA–EB system

Viscosity measurements

Viscosity measurement that is sensitive to length changes, is regarded as the least ambiguous and most critical test of DNA-binding modes in solution, and provides reliable evidence for the intercalative binding mode [32, 33]. As illustrated in Fig. 7, on increasing the amount of both test compounds, the relative viscosity of HS–DNA increased steadily, providing further evidence that both compounds bind to HS–DNA by intercalation [32, 33]. Once again, the complex shows a bigger effect than the free ligand.

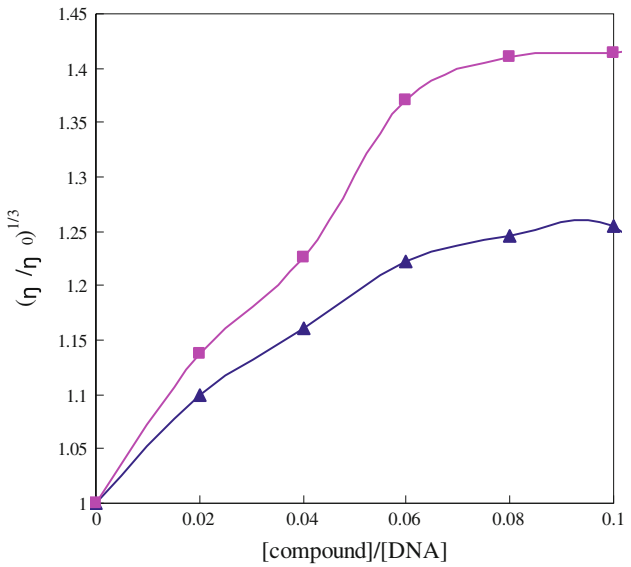

Fig. 7 Effect of the increasing amount of the two compounds (*triangle* for **L**, *diamond* for **1**) on the relative viscosity of herring sperm DNA at 298.0 (±0.1) K, [DNA] = 0.2 mM

Conclusion

A new dissymmetrical *N,N'*-bis(substituted)oxamide ligand and its tetracopper(II) complex have been synthesized and their structures were determined by single-crystal X-ray analysis. Both of the free ligand and the complex can interact with HS–DNA by intercalation, and the complex has better DNA-binding ability than the free ligand. In addition, the tetracopper(II) complex shows significant levels of cytotoxicity. These results should be valuable in understanding the binding properties of such compounds with DNA as well as laying a foundation for the rational design of novel, powerful agents for targeting nucleic acids.

Supplementary materials

Crystallographic data have been deposited at the Cambridge Crystallographic Data Centre with the deposition numbers 869922 and 869921 for H_3bhyox and the copper complex, respectively. These data can be obtained free of charge via www.ccdc.cam.ac.uk/data_request/cif.

Acknowledgments This project was supposed by the National Natural Science Foundation of China (No. 21071133), the Program for Science and Technology of Shandong Province (2011GHY 11521), and the Natural Science Foundation of Qingdao City [No. 11-2-4-1-(9)gch) and 12-1-3-52-(1)-nsh].

References

1. Zhang CX, Lippard SJ (2003) Curr Opin Chem Bio 7:481–489
2. Jamieson ER, Lippard SJ (1999) Chem Rev 99:2467–2498
3. Wong E, Giandomenico CM (1999) Chem Rev 99:2451–2466
4. Chen X, Gao F, Zhou ZX, Yang WY, Guo LT, Ji LN (2010) J Inorg Biochem 104:576–582
5. Lippert B (2000) Coord Chem Rev 200:487–516
6. Xu H, Zheng KC, Deng H, Lin LJ, Zhang QL, Ji LN (2003) New J Chem 27:1255–1263
7. Asadi M, Safaei E, Ranjbar B, Hasani L (2004) N J Chem 28:1227–1234
8. Li YT, Zhu CY, Wu ZY, Jiang M, Yan CW (2009) J Coord Chem 62(23):3795–3809
9. Ren R, Yang P, Zheng WJ, Hua ZC (2000) Inorg Chem 39:5454–5463
10. Bhat SS, Kumbhar AA, Heptullah H, Khan AA, Gobre VV, Gejji SP, Puranik VG (2011) Inorg Chem 50:545–558
11. Dhara K, Roy P, Rarha J, Manassero M, Banerjee P (2007) Polyhedron 26:4509–4517
12. Li YT, Yan CW, Guan HS (2004) Synth Met 144:69–73
13. Liu ZL, Li LC, Liao DZ, Jiang ZH, Yan SP (2005) Cryst Growth Des 5(2):783–787
14. Lu HH, Li YT, Wu ZY, Zheng K, Yan CW (2011) J Coord Chem 64:1360–1374
15. Sheldrick GM (1997) SHSLXL97, program for crystal structure refinement. University of Göttingen, Germany
16. Chand B, Ray U, Mostafa G, Lu TH, Sinha C (2004) Polyhedron 23:1669–1676
17. Geary WJ (1971) Coord Chem Rev 7:81–122
18. Ojima H, Nonoyama K (1988) Coord Chem Rev 92:85–111
19. Lin WH, Sun WL, Yang J, Shen ZQ (2008) Mater Chem Phys 112:617–623
20. Nakamoto K (1978) Infrared and raman spectra of inorganic and coordination compounds, 3rd edn. Wiley, New York
21. Camurlu P, Yilmaz A, Tatar L, Kisakürek D, Ülkü D (2005) Cryst Res Technol 40:271–276
22. Addison AW, Rao TN, Reedijk J, Rijn J, Verschoor GC (1984) J Chem Soc Dalton Trans 7:1349–1356
23. Cremer D, Pople JA (1975) J Am Chem Soc 97:1354–1358
24. Duan LM, Xie FT, Chen XM, Chen Y, Lu YK, Cheng P, Xu JQ (2006) Cryst Growth Des 6:1101–1106
25. Hernández W, Spodine E, Beyer L, Schröder U, Richter R, Ferreira J, Pavani M (2005) Bioinorg Chem Appl 3(3–4):299–316
26. Bloomfield VA, Crothers DM, Tinoco I (1974) Physical chemistry of nucleic acids. Harper and Row, New York
27. Wolfe A, Shimer GH, Meehan T (1987) Biochemistry 26:6392–6396
28. Baldini M, Belicchi-Ferrari M, Bisceglie F, Dall-Aglio PP, Pelosi G, Pinelli S, Tarasconi P (2004) Inorg Chem 43:7170–7179
29. Wu HL, Yuan JK, Bai Y, Pan GL, Wang H, Shu XB (2012) J Photochem Photobiol B107:65–72
30. Shen R, Wang P, Tang N (2009) J Fluoresc 19:1073–1082
31. Stern O, Volmer M (1919) Z Phys 20:183–188
32. Satyanarayana S, Dabrowiak JC, Chaires JB (1992) Biochemistry 31:9319–9324
33. Jin L, Yang P (1997) J Inorg Biochem 68:79–83